Journal of Engineering Physics and Thermophysics, Vol. 73, No. 6, 2000

CONDUCTION AND RADIATION OF A XENON PLASMA IN ELECTRIC-DISCHARGE PUMPING SOURCES

B. A. Barikhin*) and Yu. I. Kryshalovich

UDC 533.9.082.715+681.7.069.24

A quantitative analysis of the conditions of stabilization of the conduction of a plasma at the leading edge of an electric-discharge pulse in xenon is performed. The ranges of gas pressures and plasma temperatures in the region of stabilization are estimated. It is established that the homogeneity of the discharge plasma is the deciding factor for stabilization of its conduction. It is noted that under certain conditions self-structurization of the plasma is attained. The role of impurities in the formation of the mechanism of conduction and their influence on the plasma radiation are evaluated. Calculated data are compared with data of experiments.

In electric-discharge sources of pumping of lasers, radiation from the electric-discharge plasma is usually used to excite the active medium; the plasma serves as an alternating resistive load of the discharge circuit. Because of this, the properties of the optical radiation from the plasma are prescribed by the spectral characteristics of the active medium, first of all, by the parameters of the absorption band (band profile, character of broadening, absorption coefficient, optical density of the medium, and others). To simplify the calculations, it is convenient to go from the dimensional spectral density of the radiation energy

$$u(\nu; T) = \frac{8\pi h}{c^3} \frac{\nu^3}{\exp\left\{h\nu/kT_{\text{pl}}\right\} - 1} \tag{1}$$

to the dimensionless spectral density [1]

$$\varphi_{\text{rh}}(y, t) = \frac{u(\nu, T)}{A} = \frac{y^3}{\exp\left\{ay/t_{\text{pl}}\right\} - 1}, \tag{2}$$

which depends on the dimensionless frequency y represented in the form $\nu = y \cdot 10^{15}$ sec^{-1}, which is optimum for the optical range and on the dimensionless temperature t_{pl}, which, in problems on the pumping of optical-range electric-discharge lasers, is conveniently defined as $T_{\text{pl}} = t_{\text{pl}} \cdot 10^4$ K. In this case, the constants in (2) have the following values: $A = 6.17977 \cdot 10^{-13}$ J/(m^3·sec^{-1}) and $a = 4.7993$. For example, Fig. 1 shows the optical density of an alcoholic solution of rhodamine 6G $z_{\text{a}}(y)$ in the absorption band from $\nu_1 = 0.5 \cdot 10^{15}$ sec^{-1} to $\nu_2 = 1.5 \cdot 10^{15}$ sec^{-1}. The pumping efficiency is defined as the ratio between the intensity of the electric-discharge plasma radiation absorbed in this band

$$J_{\text{à}}(y_1, y_2, t) = \int_{y_1}^{y_2} z_{\text{à}}(y)\, \varphi_{\text{rh}}(y, t)\, dy, \tag{3}$$

and the intensity of the plasma radiation throughout the entire spectral range

---

*) Deceased.

Ya. Kupala Grodno State University, Grodno, Belarus. Translated from Inzhenerno-Fizicheskii Zhurnal, Vol. 73, No. 6, pp. 1220-1228, November–December, 2000. Original article submitted December 15, 1999.

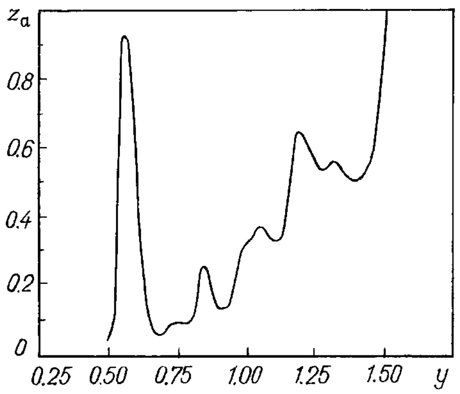

Fig. 1. Optical density of an alcoholic solution of rhodamine 6G. z_a and y, dimensionless quantities.

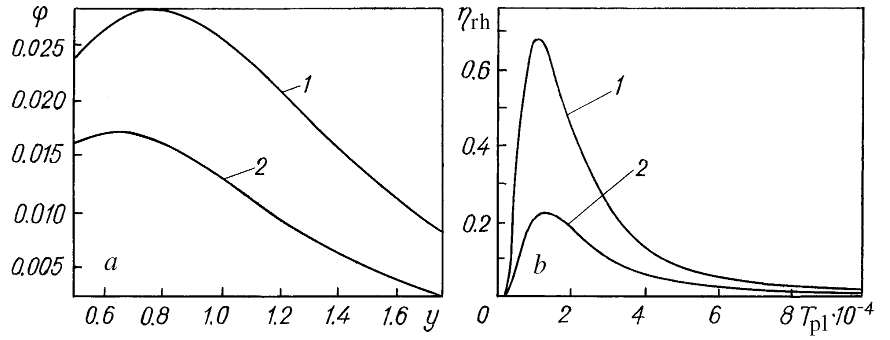

Fig. 2. Spectral density of the pumping radiation (a) and efficiency of use of the pumping-radiation energy (b) at $T_{pl} = 1.3\cdot 10^4$ K (curve 1) and $T_{pl} = 1.1\cdot 10^4$ K (curve 2).

$$J_t = \int_0^\infty \varphi_{rh}(y, t)\, dy\,. \qquad (4)$$

The dependence of this ratio

$$\eta_{rh}(t) = \frac{J_{\grave{a}}(y_1, y_2, t)}{J_t} \qquad (5)$$

on the temperature of the source is shown in Fig. 2b by curves 1 ($z_a(y) = 1$; $T_{pl} = 1.1\cdot 10^4$ K) and 2 ($z_a(y) \neq$ const; $T_{pl} = 1.3\cdot 10^4$ K). The maximum value of the ratio $\eta_{rh} \approx 0.22$ is attained at $T_{pl} \approx 1.3\cdot 10^4$ K (curve 1), the maximum value of the ratio $\eta_{rh} \approx 0.68$ without the active medium ($z_a(y) = 1$) is realized at $T_{pl} \approx 1.1\cdot 10^4$ K (curve 2). The spectral distribution of the pumping radiation $\varphi(y)$ (in dimensionless frequencies) at $T_{pl} = 1.3\cdot 10^4$ K is shown by curve 1 and, at $T_{pl} = 1.1\cdot 10^4$ K, by curve 2 in Fig. 2a. In the development of the leading edge of the excitation pulse, pumping is realized due to quite definite changes in the conduction of the discharge plasma in this time interval [2]. In order that the induced losses in the active medium of the laser be stabilized after breakdown of the interelectrode space of the pumping source, the conduction must increase rapidly (in a time of ≤ 1 μsec for a laser with a rhodamine 6G solution [3]) and, thereafter, be practically constant up to the moment when the maximum of the discharge-current strength is attained. As was shown earlier [4], the stabilization of the energy release in the active resistance of the circuit required for this purpose, with the maximum efficiency of the energy stored in the storage (≈ 0.7), is attained in the case where σ_e increases by an exponential law with an exponent $\gamma \approx 1.6$.

The conduction of a fairly heated ($t_{pl} > 1$) and fully ionized ($\alpha_e = \alpha_i = 1$) Coulomb electric-discharge plasma increases by the law $T_{pl}^{3/2}$ due to electron-ion collisions [5]:

TABLE 1. Basic Parameters of the Plasma of a Pulsed Discharge in Xenon

P_{Xe}, torr	T_{Xe}, K																					
	10^4		$1.2 \cdot 10^4$		$1.4 \cdot 10^4$		$1.6 \cdot 10^4$		$1.8 \cdot 10^4$		$2.0 \cdot 10^4$		$2.2 \cdot 10^4$		$2.4 \cdot 10^4$		$2.6 \cdot 10^4$		$2.8 \cdot 10^4$		$3.0 \cdot 10^4$	
1	616.0	63.4	828.0	69.5	1129.0	75.1	1471.9	80.2	1862.4	85.1	2300.8	89.7	2781.2	94.1	3312.8	98.3	3868.8	102.3	4519.6	016.2	5176.6	109.9
	5.3	30.4	4.4	30.4	3.8	30.4	3.3	30.4	3.0	30.4	2.7	30.4	2.4	30.4	2.2	30.4	2.0	30.4	1.9	30.4	1.8	30.4
5	115.4	28.4	165.3	31.1	119.5	33.6	294.1	35.9	373.1	38.1	460.6	40.1	556.9	42.1	663.2	44.0	778.1	45.8	902.6	47.5	1036.5	49.2
	5.3	17.8	4.4	17.8	3.8	17.8	3.3	17.8	3.0	17.8	2.7	17.8	2.4	17.8	2.2	17.8	2.0	17.8	1.9	17.8	1.8	17.8
10	57.5	20.1	82.9	22.0	113.0	23.7	147.6	25.4	186.9	26.9	230.7	28.4	278.0	29.8	331.4	31.1	389.0	32.4	451.1	33.6	518.0	34.8
	5.3	14.1	4.4	14.1	3.8	14.1	3.3	14.1	3.0	14.1	2.7	14.1	2.4	14.1	2.2	14.1	2.0	14.1	1.9	14.1	1.8	14.1
15	38.3	16.4	55.2	17.9	75.1	19.4	98.2	20.7	124.2	22.0	153.4	23.2	185.4	24.3	220.7	25.4	258.9	26.4	300.4	27.4	345.2	28.4
	5.3	12.3	4.4	12.3	3.8	12.3	3.3	12.3	3.0	12.3	2.7	12.3	2.4	12.3	2.2	12.3	2.0	12.3	1.9	12.3	1.8	12.3
20	28.8	14.2	41.4	15.5	56.3	16.8	73.5	17.9	93.3	19.0	115.3	20.1	139.3	21.0	165.3	22.0	195.6	22.9	226.1	23.7	258.7	24.6
	5.3	11.2	4.4	11.2	3.8	11.2	3.3	11.2	3.0	11.2	2.7	11.2	2.4	11.2	2.2	11.2	2.0	11.2	1.9	11.2	1.8	11.2
25	22.5	12.7	33.2	13.9	45.1	15.0	59.0	16.0	74.6	17.0	92.5	18.0	111.4	18.8	132.8	19.7	158.2	20.4	179.9	21.2	207.4	22.0
	5.3	10.4	4.4	10.4	3.8	10.4	3.3	10.4	3.0	10.4	2.7	10.4	2.4	10.4	2.2	10.4	2.0	10.4	1.9	10.4	1.8	10.4
30	19.1	11.6	27.6	12.7	37.5	13.7	49.0	14.6	62.2	15.5	76.5	16.4	92.9	17.2	110.0	17.9	129.7	18.7	150.2	19.4	172.9	20.1
	5.3	9.8	4.4	9.8	3.8	9.8	3.3	9.8	3.0	9.8	2.7	9.8	2.4	9.8	2.2	9.8	2.0	9.8	1.9	9.8	1.8	9.8
35	16.4	10.7	23.7	11.8	32.2	12.7	42.1	13.6	53.3	14.4	65.7	15.2	79.6	15.9	95.0	16.6	110.9	17.3	129.1	18.0	147.5	18.6
	5.3	9.3	4.4	9.3	3.8	9.3	3.3	9.3	3.0	9.3	2.7	9.3	2.4	9.3	2.2	9.3	2.0	9.3	1.9	9.3	1.8	9.3
40	14.4	10.0	20.7	11.0	26.0	11.9	36.8	12.7	46.6	13.5	57.7	14.2	69.5	14.9	83.2	15.6	97.5	16.2	112.6	16.8	129.7	17.4
	5.3	8.9	4.4	8.9	3.8	8.9	3.3	8.9	3.0	8.9	2.7	8.9	2.4	8.9	2.2	8.9	2.0	8.9	1.9	8.9	1.8	8.9
50	11.5	9.0	16.6	9.8	22.6	10.6	29.5	11.3	37.3	12.0	46.0	12.7	55.7	13.3	66.2	13.9	77.8	14.5	90.4	15.0	103.6	15.5
	5.3	8.2	4.4	8.2	3.8	8.2	3.3	8.2	3.0	8.2	2.7	8.2	2.4	8.2	2.2	8.2	2.0	8.2	1.9	8.2	1.8	8.2
100	5.8	6.3	8.3	7.0	11.3	7.5	14.7	8.0	18.6	8.5	23.0	9.0	27.8	9.4	33.1	9.8	38.9	10.2	45.2	10.6	51.8	11.1
	5.3	6.6	4.4	6.6	3.8	6.6	3.3	6.6	3.0	6.6	2.7	6.6	2.4	6.6	2.2	6.6	2.0	6.6	1.9	6.6	1.8	6.6

Note: Each value of T_{Xe} and P_{Xe} corresponds to four numbers: in a cell, at the top left is l_{ee}, at the top right is r_D, at the bottom left is l_Λ, and at the bottom right is l.

$$\sigma_{ei} = \frac{16\pi\varepsilon_0^2}{e^2\sqrt{2m_e}} \frac{n_e}{n_i\Lambda_{ei}} \theta_{pl}^{3/2}, \tag{6}$$

where $\varepsilon_0 = 8.854\cdot10^{-12}$ F/m is the dielectric constant; m_e and e are the mass and charge of the electron; n_e and n_i are the electron and ion concentrations, respectively; Λ_{ei} is the Coulomb logarithm for electron-ion collisions; $\theta_{pl} = k_B T_{pl}$ is the plasma temperature in energy units; $k_B = 1.38\cdot10^{-23}$ J/K is the Boltzmann constant.

At the leading edge, the temperature increases in proportion to the time of increase [2, 6] in the quantity $\theta_{pl} \sim x^b$ (b = const, it was assumed that the time is the dimensionless variable $x = \omega_0 t$, ω_0 is the frequency of the discharge-current oscillations), and b can take values from 1.5 to 2.5 according to the estimates in [6]. Because of this, the conduction increases by the law $\sigma_e \sim x^c$, where the constant c can take values from ≈ 2 to ≈ 4 according to [4, 7], i.e., in all cases, $c > \gamma$ and, in principle, the most efficient contribution of the stored energy to the electric-discharge plasma cannot be realized. However, this holds only for the law $\theta_{pl}^{3/2}$.

To stabilize the plasma conduction, it is necessary to switch on a mechanism of conduction that differs from the collisional mechanism and decreases the conduction equally effectively. Such a mechanism is provided by the known property of the Ramsauer effect [8] – an increase in the cross section of elastic scattering of "slow" electrons by neutral atoms of heavy inert gases. In this case, it is assumed that "slow" electrons are electrons with a kinetic energy from ≈0.5 to ≈10 eV, which corresponds to the values of the dimensionless brightness temperature of the plasma $0.5 \le t_{pl} \le 10$. According to the evaluations of [8-10] and measurement data obtained in experiments on determining the parameters of an electric-discharge plasma [6, 10], its conduction resulting from elastic scattering of electrons by neutral Xe atoms is determined, in the range of gas pressures $0.1 \le P_{Xe} \le 25$ torr, by the semiempirical expression

$$\sigma_{en} \approx \frac{e^2}{\sqrt{2m_e}} \frac{\alpha_i(1-\alpha_i)}{\pi a_0^2 z_{Xe}^2} \frac{\exp\{\theta_{pl}/2U_{Xe}\}}{\sqrt{\theta_{pl}}}, \tag{7}$$

where α_i is the degree of plasma ionization; z_{Xe} is the atomic number of the chemical element; a_0 is the classical radius of the first Bohr orbit; U_{Xe} is the first ionization potential of Xe.

In the case of full ionization of the plasma, this mechanism switches off; therefore, to effectively compensate for the increase in the conduction by the law $\theta^{3/2}$, it is necessary to decrease the working-gas pressure in the chosen range. This increases the nonideality of the plasma. As follows from the estimates (see Table 1), the criterion of plasma ideality

$$l_\Lambda << \bar{l} << r_D << l_{ee}, \tag{8}$$

(where l_Λ is the Landau length, m; $\bar{l}$ is the mean distance between the charged particles, m; r_D is the Debye radius, m; l_{ee} is the free path length in electron-electron collisions, m) takes the form of the ordinary inequality

$$l_\Lambda < \bar{l} < r_D < l_{ee} \tag{9}$$

and practically ceases to be fulfilled, and the strong-nonideality condition is not yet fulfilled, i.e., the plasma is weakly nonideal. Here, according to the estimates presented in Table 2, only starting with the pressure $P_{Xe} \approx 15$ torr at the temperature $T_{pl} \approx 2\cdot10^4$ K, is full ionization of the plasma attained. However, the plasma remains fairly dense, which is evidenced by the fact that at the temperature $T_{pl} \approx 1.8\cdot10^4$ K and the pressure $P_{Xe} \approx 15$ torr the frequency of the electron-atom collisions ν_{en} (in units of 10^{12} sec^{-1} in Table 2) is still ≈0.2 of the frequency of the electron-ion collisions ν_{ei} (in units of 10^{12} sec^{-1}).

After full ionization of the plasma, its conduction $\sigma_e = \sigma_{ei} + \sigma_{en}$ (in units of $(\Omega\cdot m)^{-1}$ in Table 2) is described just by the law $\sigma_{ei} \sim \theta^{3/2}$. Experiment and calculation showed that in the ranges of gas pressures $1 \le P_{Xe} \le 10$ torr and plasma temperatures $10^4 \le T_{pl} \le 2\cdot10^4$ K this regularity is fairly distinctly compensated for by the Ramsauer effect. It is clear that scattering will be more effective, the greater the number of plasma

TABLE 2. Degree of Ionization, Frequencies of Electron-Ion and Electron-Atom Collisions, and Electronic Conduction of the Plasma of a Pulsed Discharge in Xenon

P_{Xe}, torr	T_{Xe}, K																					
	10^4		$1.2 \cdot 10^4$		$1.4 \cdot 10^4$		$1.6 \cdot 10^4$		$1.8 \cdot 10^4$		$2.0 \cdot 10^4$		$2.2 \cdot 10^4$		$2.4 \cdot 10^4$		$2.6 \cdot 10^4$		$2.8 \cdot 10^4$		$3.0 \cdot 10^4$	
1	0.175	0.171	0.20	0.130	0.225	0.103	0.249	0.085	0.272	0.071	0.294	0.060	0.316	0.0752	0.337	0.046	0.358	0.041	0.378	0.036	0.398	0.033
	0.031	0.399	0.036	0.421	0.042	0.437	0.046	0.450	0.051	0.460	0.056	0.466	0.060	0.471	0.065	0.473	0.070	0.474	0.074	0.472	0.079	0.470
5	0.252	0.855	0.288	0.651	0.324	0.518	0.358	0.423	0.391	0.354	0.424	0.302	0.455	0.262	0.486	0.230	0.516	0.204	0.545	0.183	0.574	0.164
	0.047	1.811	0.057	1.875	0.067	1.907	0.076	1.925	0.086	1.922	0.096	1.902	0.106	1.875	0.118	1.834	0.130	1.785	0.142	1.728	0.157	1.664
10	0.411	1.712	0.471	1.302	0.529	1.035	0.584	0.847	0.638	0.708	0.691	0.604	0.742	0.524	0.792	0.460	0.841	0.408	0.890	0.365	0.937	0.329
	0.090	2.854	0.115	2.787	0.143	2.660	0.175	2.496	0.214	2.287	0.261	2.042	0.322	1.777	0.407	1.485	0.532	1.174	0.636	0.836	1.141	0.492
15	0.628	3.236	0.720	1.953	0.803	1.553	0.894	1.269	0.976	1.063	1.0	0.907	1.0	0.786	1.0	0.690	1.0	0.612	1.0	0.548	1.0	0.494
	0.158	2.703	0.259	2.212	0.374	1.668	0.585	0.954	1.135	0.227	1.658	0	1.909	0	2.174	0	2.452	0	2.740	0	3.040	0
20	0.886	3.425	1.0	2.604	1.0	2.070	1.0	1.692	1.0	1.416	1.0	1.209	1.0	1.048	1.0	0.920	1.0	0.816	1.0	0.730	1.0	0.658
	0.442	1.104	0.768	0	0.966	0	1.182	0	1.412	0	1.654	0	1.909	0	2.175	0	2.451	0	2.741	0	3.040	0
25	1.0	4.273	1.0	3.257	1.0	2.591	1.0	2.114	1.0	1.770	1.0	1.510	1.0	1.311	1.0	1.149	1.0	1.020	1.0	0.912	1.0	0.822
	0.585	0	0.768	0	0.966	0	1.182	0	1.412	0	1.654	0	1.909	0	2.175	0	2.451	0	2.741	0	3.040	0
30	1.0	5.128	1.0	3.906	1.0	3.106	1.0	2.538	1.0	2.128	1.0	1.815	1.0	1.572	1.0	1.379	1.0	1.224	1.0	1.095	1.0	0.987
	0.585	0	0.768	0	0.966	0	1.182	0	1.412	0	1.654	0	1.909	0	2.175	0	2.451	0	2.741	0	3.040	0
35	1.0	5.988	1.0	4.545	1.0	3.623	1.0	2.958	1.0	2.475	1.0	2.114	1.0	1.835	1.0	1.610	1.0	1.428	1.0	1.277	1.0	1.151
	0.585	0	0.768	0	0.966	0	1.182	0	1.412	0	1.654	0	1.909	0	2.175	0	2.451	0	2.741	0	3.040	0
40	1.0	6.849	1.0	5.208	1.0	4.132	1.0	3.378	1.0	2.833	1.0	2.415	1.0	2.096	1.0	1.838	1.0	1.613	1.0	1.460	1.0	1.316
	0.585	0	0.768	0	0.966	0	1.182	0	1.412	0	1.654	0	1.909	0	2.175	0	2.451	0	2.741	0	3.040	0
50	1.0	8.547	1.0	6.494	1.0	5.181	1.0	4.237	1.0	3.546	1.0	3.021	1.0	2.625	1.0	2.229	1.0	2.041	1.0	1.825	1.0	1.645
	0.585	0	0.768	0	0.966	0	1.182	0	1.412	0	1.654	0	1.909	0	2.175	0	2.451	0	2.741	0	3.040	0
100	1.0	17.24	1.0	12.99	1.0	10.31	1.0	8.479	1.0	7.092	1.0	6.061	1.0	5.236	1.0	4.608	1.0	4.082	1.0	3.650	1.0	3.289
	0.585	0	0.768	0	0.966	0	1.182	0	1.412	0	1.654	0	1.909	0	2.175	0	2.451	0	2.741	0	3.040	0

Note: Each value of T_{Xe} and P_{Xe} corresponds to four numbers: in a cell, at the top left is α_i, at the top right is ν_{ei}, at the bottom left is σ_e, and at the bottom right is ν_{en}.

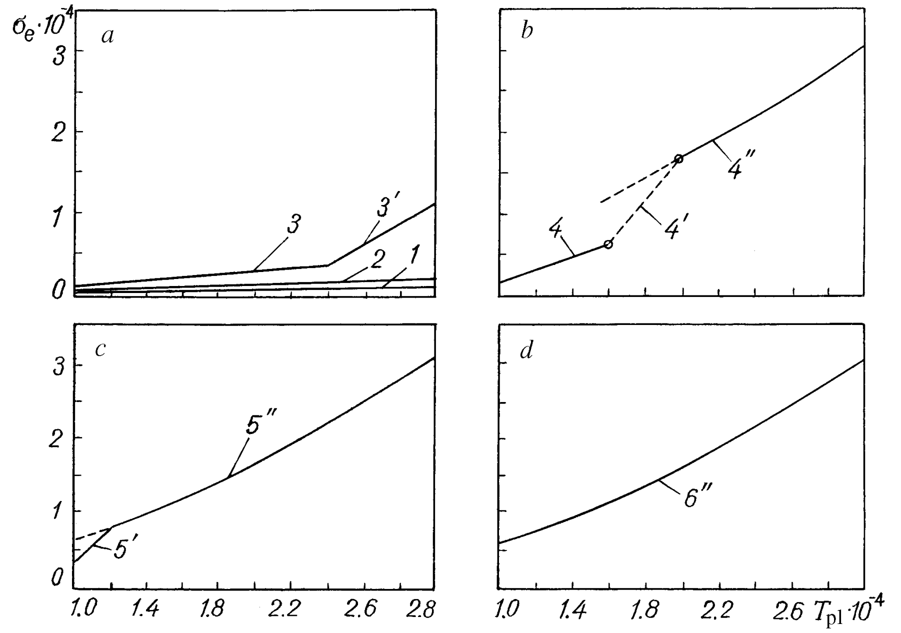

Fig. 3. Dependence of the electronic conduction of the plasma σ_e on the temperature at P_{Xe} = 1 torr (straight line 1), P_{Xe} = 5 torr (straight line 2), P_{Xe} = 10 torr (straight line 3) (a), P_{Xe} = 15 torr (b), P_{Xe} = 20 torr (c), and P_{Xe} = 25 torr (d). σ_e, S; T_{pl}, K.

electrons that have an energy from 0.5 to 10 eV, which corresponds to the position of the maximum of the Maxwell distribution of the electron component within the range $10^4 \leq T_e^{max} \leq 10^5$ K. At smaller values of T_e^{max} the number of electrons with the energy required for resonance scattering is significantly decreased. As T_e^{max} increases, an increasing number of electrons fail to interact with the potential well of an Xe atom. The number of electrons scattered by the well can be increased by two independent means: first, by increasing the working-gas pressure until concentration saturation of the Ramsauer effect by the plasma electrons occurs; second, by increasing the temperature of the plasma in the discharge space of the pumping source to values at which the plasma is still partially ionized. According to the data in Table 2, necessary conditions for stabilization are realized in the ranges of xenon pressures $1 \leq P_{Xe} \leq 10$ torr and plasma temperatures $10^4 \leq T_{pl} \leq 2 \cdot 10^4$ K. This conclusion is supported by the results of the measurements in [6, 10].

A noteworthy feature of the compensation is the change from one mechanism of conduction to another. An increase in the voltage applied to the interelectrode space produces the following effects. In a comparatively weak external field, up to attainment of concentration saturation of the Ramsauer effect directed charge transfer is predominantly performed by electrons participating in thermal motion. Because of this, the process of relaxation of scattered electrons will be practically equilibrium in character and the regime of mixed Ramsauer and collisional conduction of the plasma, represented by straight lines 1 (P_{Xe} = 1 torr), 2 (P_{Xe} = 5), and 3 (P_{Xe} = 10) in Fig. 3a and straight line 4 (P_{Xe} = 15) in Fig. 3b, corresponds to mutual compensation of these two mechanisms. When the strength of the external field reaches a certain critical value that is conveniently expressed in units of temperature, $T'_{2cr} = 2.4 \cdot 10^4$ for P_{Xe} = 10 torr and $T'_{1cr} = 1.6 \cdot 10^4$ K for P_{Xe} = 15 torr, scattered electrons are also involved in charge transfer. The mechanism of mixed conduction becomes thermodynamically unstable (straight lines $3'$ in Fig. 3a, $4'$ in Fig. 3b, and $5'$ in Fig. 3c) since it cannot provide directed transfer of charge that is increased according to the increase in the voltage, i.e., a change to a thermodynamically stable regime (curves $4''$ in Fig. 3b, $5''$ in Fig. 3c, and $6''$ in Fig. 3d) that is more favorable for such an increase occurs. The nonanalytic behavior (break) of the coefficient of transfer (conduction) at the critical plasma temperatures T'_{cr} is analogous to the behavior of thermodynamic functions in a phase transition of the second kind, in particular, when a gas passes to a state of full ionization. Such a state arises spontaneously and is cooperative in character [11]. A jump-like increase in the conduction can arise under the considered conditions only from simultaneous (cooperative) involvement of the scattered Ramzauer electrons in the

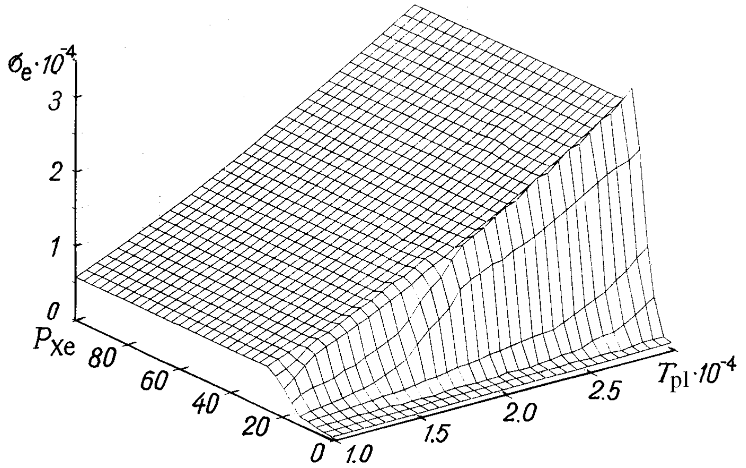

Fig. 4. Dependence of the electronic conduction of the plasma on the plasma temperature and the xenon pressure. P_{Xe}, torr.

charge transfer. In this case, the electric field of the gas ions in the plasma must be self-structurized by the moment of involvement, which in turn will lead to "metallizing" of the plasma, in part, and a jump-like increase in its conduction. In the states $T''_{5\mathrm{cr}}$ and $T''_{4\mathrm{cr}}$ the metallic structure formed will decompose because of its overheating.

This model of a self-organizing plasma is supported by the estimates given in Fig. 4, where the plasma conduction is plotted as a function of the working-gas pressure P_{Xe} and the plasma temperature T_{pl}, which is directly related to the value of the energy stored in the discharge-circuit storage through the dependence on the working voltage U_0 [6, 10] ($T_{\mathrm{pl}} \sim \sqrt{U_0}$) and, correspondingly, on the strength of the electric field between the electrodes of the discharge space. On the surface $\sigma_{\mathrm{e}}(P_{\mathrm{Xe}}; T_{\mathrm{pl}})$ (see Fig. 4) we can separate a region conventionally bounded by the values $1 \le P_{\mathrm{Xe}} \le 18$ torr and $10^4 \le T_{\mathrm{pl}} \le 2 \cdot 10^4$ K, which represents a plateau of $\sigma_{\mathrm{e}} \approx 0.16 \cdot 10^4$ S. It is seen that the shift of the conduction from the plateau to other regions is jump-like in character in the range of gas pressures $18 \le P_{\mathrm{Xe}} \le 30$ torr. Consequently, in the range found, self-organization of the discharge plasma must occur.

It is necessary to indicate immediately two circumstances limiting the degree of generality of the results of the analysis performed, which are supported by the experimental data of [6, 10]. First, comparison of the contribution of electron-ion collisions and the Ramsauer effect to the formation of the electronic-conduction mechanism can be brought to the level of quantitative evaluations only in a homogeneous electric-discharge plasma, first of all, because of a different form of the dependence of σ_{ei} and σ_{en} on θ_{pl}, the independence of the collisional conduction from the electron concentration in the single-ionization approximation, and the dependence of the Ramsauer conduction on the concentration of neutral atoms (the degree of plasma ionization). Second, the existence of easily ionized metal impurities arising as a result of electrode erosion that can even be observed visually distorts the basic plasma parameters [5, 6]. Furthermore, the presence of impurities in the working gas for which the Ramsauer effect is absent leads to smoothing of the breaks at the critical points of the electronic-conduction curves and, with a high concentration of impurities, can suppress the Ramsauer mechanism so much that self-organization of the plasma will not occur.

The influence of impurities on the radiation of an electric-discharge plasma is even more substantial [5]. For xenon, the energy of the braking radiation $W_{\mathrm{br}} \sim n_{\mathrm{e}} n_{\mathrm{i}} z^2 / \sqrt{T_{\mathrm{e}}}$ equals the energy of the recombination radiation $W_{\mathrm{rec}} \sim n_{\mathrm{e}} n_{\mathrm{i}} z_{\mathrm{i}}^4 / \sqrt{T_{\mathrm{e}}}$ at the plasma temperature $T_{\mathrm{pl}} \approx 10^4$ K. Here, n_{i} and z_{i} are the concentration and the charge of the positive ions, T_{e} is the temperature of the electronic component. The presence of easily ionized impurities significantly changes n_{i}, n_{e}, and z_{i} and leads to marked disturbance of the balance between the braking and recombination radiations, for example, the existence of doubly ionized metal atoms in the plasma can, in the case of a significant concentration of them (even near the electrodes), increase the recombination radiation intensity by approximately an order of magnitude. Thus, a situation can occur where the recombination-radiation mechanism works in the near-electrode volume of the discharge space, and the braking mechanism works in the remaining portion of the plasma column. This points to the fact that there is no way to construct a model of xenon-plasma radiation in the region $10^4 \leq T_{\text{pl}} \leq 2\cdot 10^4$ K even at the level of qualitative evaluations; construction of a model of the radiation from a plasma without impurities accomplishes nothing, since the degree of generality of such a model is no higher than the degree of generality of any other model. Because of this, reliable values of the xenon-plasma parameters in the indicated range can be obtained only by way of physical measurements. The single reliably established result of both the analysis [5] and the experiments performed earlier [6, 10] can be that the radiation spectrum of a xenon plasma in this region is with good accuracy continuous and, in the visible and near-UV and IR regions, is practically identical to the radiation spectrum of a blackbody. Because of this, energy measurements of the plasma radiation can be performed using the simplest calorimetric methods.

Direct calorimetric and calibration measurements in a discharge circuit with a capacitance of 120 μF and an inductance of 0.3 μH whose load was a coaxial flash lamp [6] have shown that the brightness temperature of the plasma integrated over the pulse is related to the working voltage across the storage U_0 by the relation

$$T_{\text{pl}} \approx B\sqrt{U_0} \tag{10}$$

for $B \approx 1.06\cdot 10^2$ K/V$^{1/2}$, and processing of spectrochronograms made it possible to determine the relation between the brightness temperature at the pumping-pulse maximum T_{max} and the working voltage across the storage:

$$T_{\text{max}} \approx C\sqrt{3U_0} \tag{11}$$

for $C = 10^2$ K/V$^{1/2}$. Comparison of the coefficients in (10) and (11) provides support for the above assumption of a fairly rapid increase in the brightness temperature at the leading edge of the pumping pulse of an electric-discharge laser.

NOTATION

T_{pl}, plasma temperature; T_{e}^{max}, maximum temperature of the electronic component of the plasma; T'_{cr}, critical plasma temperature; T_{max}, temperature at the pumping-pulse maximum; t_{pl}, dimensionless temperature of the plasma; t, dimensionless temperature; u, spectral density of the plasma-radiation energy; U_0, initial voltage across the storage; φ_{rh}, dimensionless spectral density of the plasma-radiation energy; $\varphi(y)$, spectral distribution of the pumping radiation; ν, frequency; y, dimensionless frequency; J_{t}, plasma- radiation intensity throughout the entire spectral range; J_{a}, intensity of the radiation absorbed by the active medium; η_{rh}, pumping efficiency (ratio $J_{\text{t}}/J_{\text{a}}$); γ, exponential parameter; $z_{\text{a}}(y)$, optical density of the active medium; σ_{ei}, electron-ionic conduction of the plasma; σ_{en}, electron-atomic conduction of the plasma; σ_{e}, electronic conduction of the plasma; ν_{ei}, frequency of electron-ion collisions; ν_{en}, frequency of electron-atom collisions; x, dimensionless time; P_{Xe}, xenon pressure; W_{br}, energy of the xenon braking radiation; W_{rec}, energy of the xenon recombination radiation; a, A, B, and C, coefficients; h, Planck constant; c, velocity of light. Subscripts: a, active medium; rh, rhodamine 6G; Xe, xenon; cr, critical; br, braking; rec, recombination; pl, plasma; e, electron; i, ion; n, neutral; max, maximum; 0, initial value; 1, 2, 3, and 4, enumeration indices; t, total; ′ and ″, unsteady and steady mechanisms of conduction.

REFERENCES

1. P. A. Apanasevich and V. S. Aizenshtadt, *Tables of Distribution of Energy and Photons in the Equilibrium-Radiation Spectrum* [in Russian], Minsk (1971).
2. I. S. Marshak (ed.), *Pulsed Light Sources* [in Russian], Moscow (1978).

3. A. N. Rubinov and T. I. Smol’skaya, in: B. I. Stepanov and A. M. Samson (eds.), *Quantum Electronics and Laser Spectroscopy* [in Russian], Minsk (1971), pp. 33-80.
4. B. A. Barikhin and Yu. I. Kryshalovich, *Inzh.-Fiz. Zh.*, **73**, No. 5, 953-961 (2000).
5. L. A. Artsimovich and R. Z. Sagdeev, *Plasma Physics for Physicists* [in Russian], Moscow (1979).
6. F. N. Baltakov and B. A. Barikhin, *Kvant. Élektronika*, **2**, No. 4, 822-826 (1975).
7. A. A. Bakeev, *Electrical and Optical Properties of a High-Pressure Pulsed Xenon Discharge*, Candidate’s Dissertation in Physical and Mathematical Sciences, Moscow (1970).
8. N. Mott and H. Massey, in: *Theory of Atomic Collisions* [Russian translation], Moscow (1958), pp. 93-118.
9. A. F. Akkerman, *Modeling of the Trajectories of Charged Particles in Matter* [in Russian], Moscow (1991).
10. F. N. Baltakov, B. A. Barikhin, V. G. Kornilov, et al., *Zh. Tekh. Fiz.*, **42**, No. 7, 1459-1461 (1972).
11. W. Ebeling, *Formation of Structures in Irreversible Processes* [Russian translation], Moscow (1979).